AFCRL-66-551

IMPEDANCE OF A FINITE INSULATED CYLINDRICAL ANTENNA IN A COLD PLASMA WITH A LONGITUDINAL MAGNETIC FIELD

by

J. Galejs

APPLIED RESEARCH LABORATORY
SYLVANIA ELECTRONIC SYSTEMS
A Division of Sylvania Electric Products Inc.
40 SYLVAN ROAD, WALTHAM, MASSACHUSETTS 02154

Contract No. AF19(628)-5718
Project No. 4642
Task No. 464202
Scientific Report No. 2

25 July 1966

Prepared for

AIR FORCE CAMBRIDGE RESEARCH LABORATORIES
Office of Aerospace Research
United States Air Force
Bedford, Massachusetts

AFCRL-66-551

IMPEDANCE OF A FINITE INSULATED CYLINDRICAL ANTENNA IN A COLD PLASMA WITH A LONGITUDINAL MAGNETIC FIELD

by

J. Galejs

APPLIED RESEARCH LABORATORY
SYLVANIA ELECTRONIC SYSTEMS
A Division of Sylvania Electric Products Inc.
40 SYLVAN ROAD, WALTHAM, MASSACHUSETTS 02154

Contract No. AF19(628)-5718

Project No. 4642

Task No. 464202

Scientific Report No. 2

25 July 1966

Prepared for

AIR FORCE CAMBRIDGE RESEARCH LABORATORIES
Office of Aerospace Research
United States Air Force
Bedford, Massachusetts

IMPEDANCE OF A FINITE INSULATED CYLINDRICAL ANTENNA IN A COLD PLASMA WITH A LONGITUDINAL MAGNETIC FIELD

by

Janis Galejs

Applied Research Laboratory
Sylvania Electronic Systems
A division of Sylvania Electric Products Inc.
Waltham, Massachusetts 02154

ABSTRACT

A variational formulation is developed for the impedance of a finite cylindrical antenna embedded in a dielectric cylinder, which is surrounded by a magneto-ionic medium (cold electron plasma) with the static magnetic field impressed in a direction parallel to the antenna axis. Closed form expressions are obtained in the limit of low frequencies, and for short antennas in a uniaxial medium. The impedance of a short antenna is nearly the same as for an assumed triangular current distribution, except that further resonances are observed in the vicinity of the gyro frequency, where the antenna becomes electrically long. These resonances may be shifted to frequencies exceeding the gyro frequency in the presence of an insulating layer around the antenna. For very thin insulating layers the wave number of the variationally approximated current distribution is to the first order equal to $\sqrt{\epsilon_1}\, k_o$ (ϵ_1 is the leading diagonal element of the permittivity matrix), where the gyro frequency may be both smaller or larger than the plasma frequency. However this approximation does not apply to current distributions along the insulated antenna. The present calculations are also compared with earlier work on antenna impedances.

TABLE OF CONTENTS

LIST OF ILLUSTRATIONS

Impedance of a finite insulated cylindrical antenna in a cold plasma with a longintudinal magnetic field

by

Janis Galejs

1. INTRODUCTION

A large number of authors have been concerned with radiation from various sources in a magnetoionic medium.[1-12] The impedance of a short current element has been considered using the quasi-static approximation,[13-15] and integral expressions for the radiation resistance of elementary antennas have been developed.[16-26]

The impedance of a linear antenna has been also considered, but there are numerous discrepancies between the results of various investigators. The impedance of the cylindrical antenna with an arbitrary directed static magnetic field has been computed by Ament et al.[27] for frequencies above the plasma or cyclotron frequencies. This impedance formulation assumes that the current distribution along the antenna is sinusoidal with an assumed wave number. Staras[28] has computed the impedance of a short antenna (which is either parallel or perpendicular to the static magnetic field) based on the concept of a volumetric current distribution which is selected such that the evaluation of the impedance integrals is reasonably practical. Numerical results are presented only for frequencies which are much lower than the plasma or the cyclotron frequencies, and for thin antennas parallel to the magnetic field the antenna reactance is inductive and it is 1-1/2 to 8 times larger than the resistance.

Antenna impedance is also discussed in two recent reports. Brandstatter and Penico[29] consider an arbitrary direction of the static magnetic field, and assume that the antenna current can be represented as the sum of two sine waves.

The complex wave numbers for these two trial functions are the same as for the plane waves (ordinary and extra-ordinary) propagating along the antenna axis. Only numerical results for frequencies which are much lower than the plasma or cyclotron frequency are presented. The antenna reactance for an orientation parallel to the static magnetic field is less than 10^{-2} Ohms for antennas of the length from 10 to 30 meters at the frequency of 18 Kc/s and the resistance part of the antenna impedance is 3 to 4 orders of magnitude lower. This seems to be in contradiction with the results of Staras.[28] Ament et al.[30] also consider an arbitrary direction for the static magnetic field. It is indicated that the antenna impedance is capacitive for antennas parallel to the magnetic field in the VLF range. For the antenna parameters investigated by Brandstatter and Penico[29] the antenna impedance exceeds 1000 Ohms in magnitude (Table 2), and the impedance has a significant real part. Some further calculations (Table 4) show also an inductive impedance. Based on the stationary character of an approximate impedance expression Ament et al.[30] obtained a simple estimate for a propagation coefficient of the current distribution along the antenna. However in the low frequency limit this impedance expression differs significantly from quasi-stationary impedance expressions derived by others.[15]

The discussion above indicates that further work is needed to clarify the impedance characteristics of antennas in a magnetoionic medium. The impedance of a linear flat strip antenna in the presence of an arbitrary stratified isotropic dielectric has been computed recently, and these results have been compared with experimental data.[31] In the present paper a basically similar variational formulation will be applied to a cylindrical antenna geometry. The antenna current is assumed to flow along the surface of a cylindrical shell of length '2 ℓ' and radius 'a', which is embedded in the center of a dielectric region of radius 'b' within a magnetoionic medium with the static magnetic field in a direction parallel to the antenna axis. The dielectric cylinder is assumed to be either an actual

dielectric or to approximate the effects of an ion sheath around the antenna. Such a region, depleted of electrons has been shown to affect the antenna characteristics particularly for frequencies below the plasma frequency.[26] The field expressions in the anisotropic medium are derived using one dimensional Fourier transforms. The considerations are restricted to a slightly lossy medium and the radiation condition requires only that the fields are exponentially attenuated at large distances from the sources. The fields are expressed in terms of Bessel functions of complex argument and the antenna impedance is formulated after satisfying the boundary conditions at the surface of the current filament and at the interface between the dielectric and the plasma. The antenna impedance is computed using a two-term trial function for the antenna current. The trial functions are assumed to be two sine functions which will be specified in the later discussion. For antennas of finite radius the impedance is made available in numerical form only. However for vanishingly thin antennas closed form expressions are derived, in the low frequency limit, for short antennas in a uniaxial medium, and for half wave antennas in free space. The numerical results are compared with the earlier work of others on the same problem.

2. FIELD EXPRESSIONS IN THE COLD ELECTRON PLASMA MEDIUM

Assuming a (suppressed) $\exp(-i\omega t)$ harmonic time dependence of the fields for a source free medium the electric and magnetic vectors $\underline{E}$ and $\underline{H}$ satisfy the Maxwell's equations

$$\nabla \times \underline{E} = i\omega\mu_o \underline{H} \tag{1}$$

$$\nabla \times \underline{H} = -i\omega\epsilon_o \underline{\underline{\epsilon}} \cdot \underline{E} \tag{2}$$

where μ_o and ϵ_o are the permeability and permittivity of free space respectively. For a z-directed magnetic field the dyadic permittivity is of the form traditionally used in the classical magnetoionic theory,

$$\underline{\underline{\epsilon}} = \begin{bmatrix} \epsilon_1 & i\epsilon_2 & 0 \\ -i\epsilon_2 & \epsilon_1 & 0 \\ 0 & 0 & \epsilon_3 \end{bmatrix} \tag{3}$$

where

$$\epsilon_1 = 1 + \frac{\omega_p^2 (\omega+i\nu)/\omega}{\omega_c^2 - (\omega+i\nu)^2} \tag{4}$$

$$\epsilon_2 = - \frac{\omega_p^2 \omega_c/\omega}{\omega_c^2 - (\omega+i\nu)^2} \tag{5}$$

$$\epsilon_3 = 1 - \frac{\omega_p^2}{\omega(\omega+i\nu)} \tag{6}$$

where ν is the effective collision frequency and where the plasma frequency ω_p and the cyclotron frequency ω_c of electrons are defined in terms of the electron density N, charge e, mass m and the applied static magnetic induction B_o as $\omega_p^2 = e^2N/(m\epsilon_o)$ and $\omega_c = |e|B_o/m$. Because of the symmetry of the excitation the field components will be independent of ϕ and they are related to their Fourier transforms over the z coordinate by

$$F_{ij}(\rho,z) = \frac{1}{2\pi} \int_{-\infty}^{\infty} \bar{F}_{ij}(\rho,w)\, e^{iwz}\, dw \tag{7}$$

where F = E or H, i = ρ, ϕ or z and where subscripts j denote particular modes of propagation. A substitution of (7) into (1) and (2) gives the following relations between the transformed field components

$$i\omega\mu_o \bar{H}_\rho = - iw \bar{E}_\phi \tag{8}$$

$$i\omega\mu_o \bar{H}_\phi = - \frac{\partial}{\partial\rho} \bar{E}_z + iw \bar{E}_\rho \tag{9}$$

$$i\omega\mu_o \bar{H}_z = \frac{1}{\rho} \frac{\partial}{\partial\rho} (\rho \bar{E}_\phi) \tag{10}$$

$$-iw \bar{H}_\phi = - i\omega\epsilon_o(\epsilon_1 \bar{E}_\rho + i\epsilon_2 \bar{E}_\phi) \tag{11}$$

$$iw \bar{H}_\rho - \frac{\partial}{\partial\rho} \bar{H}_z = - i\omega\epsilon_o (-i\epsilon_2 \bar{E}_\rho + \epsilon_1 \bar{E}_\phi) \tag{12}$$

$$\frac{1}{\rho} \frac{\partial}{\partial\rho} (\rho \bar{H}_\phi) = - i\omega\epsilon_o \epsilon_3 \bar{E}_z \tag{13}$$

where the arguments (ρ,w) and the subscripts j have been omitted. The transverse field components of (8), (9), (11) and (12) can be expressed in terms of $\bar{E}_z$ and $\bar{H}_z$ as

$$\bar{E}_\rho = \frac{1}{D}\left[- (\epsilon_1 k_o^2 - w^2)\, iw \frac{\partial}{\partial\rho}\, \bar{E}_z + \omega\mu_o\, \epsilon_2\, k_o^2 \frac{\partial}{\partial\rho} \bar{H}_z \right] \tag{14}$$

$$\bar{E}_\phi = \frac{1}{D}\left[\epsilon_2 k_o^2\, w \frac{\partial}{\partial\rho}\, \bar{E}_z + i\omega\mu_o (\epsilon_1 k_o^2 - w^2) \frac{\partial}{\partial\rho}\, \bar{H}_z \right] \tag{15}$$

$$\bar{H}_\rho = \frac{w}{\omega\mu_o D}\left[- \epsilon_2 k_o^2\, w \frac{\partial}{\partial\rho} \bar{E}_z - i\omega\mu_o\, (\epsilon_1 k_o^2 - w^2) \frac{\partial}{\partial\rho}\, \bar{H}_z \right] \tag{16}$$

$$\bar{H}_\phi = \frac{1}{i\omega\mu_o D}\left\{ \left[-D + w^2\, (\epsilon_1 k_o^2 - w^2) \right] \frac{\partial}{\partial\rho} \bar{E}_z + i\omega\mu_o \epsilon_2 k_o^2 \frac{\partial}{\partial\rho} \bar{H}_z \right\} \tag{17}$$

where

$$D = \epsilon_2^2\, k_o^4 - (\epsilon_1 k_o^2 - w^2)^2 \tag{18}$$

and $k_o = \omega\sqrt{\mu_o \epsilon_o}$. Substitution of (14) to (17) into (10) and (13) gives two coupled wave equations

$$\left[- D + w^2\, (\epsilon_1 k_o^2 - w^2) \right] \mathcal{D}\, \bar{E}_z + \epsilon_2 k_o^2 w\, i\omega\mu_o\, \mathcal{D}\, \bar{H}_z = k_o^2\, \epsilon_3\, D\, \bar{E}_z \tag{19}$$

$$\epsilon_2 k_o^2 w\, \mathcal{D}\, \bar{E}_z + i\omega\mu_o (\epsilon_1 k_o^2 - w^2) \mathcal{D} \bar{H}_z = i\omega\mu_o\, D\, \bar{H}_z \tag{20}$$

where the operator $\mathcal{D}$ is defined as

$$\mathcal{D} = \frac{1}{\rho} \frac{\partial}{\partial\rho} \left(\rho \frac{\partial}{\partial\rho} \right) \tag{21}$$

Substituting $\mathcal{D}\, \bar{H}_z$ of (20) in (19) $\bar{H}_z$ is related to $\bar{E}_z$ by

$$i\omega\mu_o\, \epsilon_2\, w\, \bar{H}_z = \epsilon_1\, \mathcal{D}\bar{E}_z + \epsilon_3\, (\epsilon_1 k_o^2 - w^2)\, \bar{E}_z \tag{22}$$

This equation for $\bar{H}_z$ can be differentiated and substituted in (19) which gives the following fourth order differential equation

$$a\, \mathcal{D}^2\, \bar{E}_z + b\, \mathcal{D}\bar{E}_z + c\, \bar{E}_z = 0 \tag{23}$$

where

$$a = \epsilon_1 k_o^2 \tag{24}$$

$$b = k_o^2 \left[k_o^2(\epsilon_1^2 - \epsilon_2^2 + \epsilon_1\epsilon_3) - w^2(\epsilon_1 + \epsilon_3) \right] \tag{25}$$

$$c = - \epsilon_3 k_o^2 D \tag{26}$$

After carrying out the differentiations indicated by the operator (21), the resulting equation can be exhibited as a sum of a fourth order differential equation and a second order differential equation (equations (4.26) and (2.162.1a) respectively of Kamke[32]). Both differential equations have the Hankel functions of order zero $H_o^{(m)}(\beta\rho)$ as common solutions (m = 1 or 2), if β^2 satisfies the quadratic equation

$$a\beta^4 - b\beta^2 + c = 0 \tag{27}$$

The arguments of the Hankel functions for both differential equations become identical and the solutions of (23) have the form

$$\bar{E}_z = B(w)\, H_o^{(m)}(\beta\rho) \tag{28}$$

This result can be verified by direct substitution of (28) in (23) when noting that $\nabla H_o^{(m)}(\beta\rho) = - \beta^2 H_o^{(m)}(\beta\rho)$. The solutions of (27) are given by

$$\beta^2 = \frac{b \pm \sqrt{b^2 - 4ac}}{2a} \tag{29}$$

For w = 0 the above solutions β correspond to purely radial wave propagation in a direction transverse to the z-axis. The two solutions of (29) are now simplified to

$$\beta^2 = \begin{cases} \epsilon_3 k_o^2 \\ (\epsilon_1^2 - \epsilon_2^2)\, k_o^2/\epsilon_1 \end{cases} \tag{30}$$

Following a convention used in the past[8] the solution with a plus sign in (29) which gives $\beta^2 = \epsilon_3 k_o^2$ for w = 0 is denoted as an ordinary wave (subscript j= +) and the other solution is denoted as the extraordinary wave (j= -). The β = 0 solutions of (28) represent plane waves propagating in the z-direction with wave numbers

$$w_{\pm} = k_o \sqrt{\epsilon_1 \pm \epsilon_2} \tag{31}$$

In the presence of strong magnetic fields $\epsilon_2 \to 0$, and the anisotropic medium becomes uniaxial with $\epsilon_3 \neq \epsilon_1$. The two solutions of (29) become

$$\beta_+^2 = \epsilon_3(k_o^2 - w^2/\epsilon_1) \tag{32}$$

$$\beta_-^2 = \epsilon_1 k_o^2 - w^2 \tag{33}$$

Equations (32) and (33) apply also to isotropic media when $\epsilon_2 = 0$ and $\epsilon_3 = \epsilon_1$. The ordinary wave (32) corresponds now to TM field components which satisfy the wave equation (19). The extraordinary wave (33) has TE field components and it satisfies the wave equation (20). Obviously there is no coupling between TE and TM modes when $\epsilon_2 = 0$. For a lossy plasma β^2 will be generally complex and the sign of β can be determined from the requirement that field components should decay for large values of ρ. $\mathrm{Im}(\beta)$ should be positive if Hankel functions of the first kind (m=1) are used for the solutions (27).

In an anisotropic medium with finite magnetic field $\epsilon_2 \neq 0$, and the field components $\bar{E}_{zj}$ and $\bar{H}_{zj}$ for a given mode j are coupled. The coupling is characterized by the admittance

$$Y_j = \frac{\bar{H}_{zj}}{\bar{E}_{zj}} \tag{34}$$

It is computed after substituting (28) in (22) as

$$Y_j = -\frac{1}{i\omega\mu_o} \frac{\epsilon_1(\beta_j^2 - \epsilon_3 k_o^2) + \epsilon_3 w^2}{\epsilon_2 w} \tag{35}$$

Substituting (29) in (35) and letting $\epsilon_2 \to 0$, $Y_+ \sim \epsilon_2^2/\epsilon_2 \to 0$ and $\bar{H}_{z+} = 0$ due to an excitation by $\bar{E}_{z+}$. Similarly it is seen that $|Y_-| \to \infty$ and $\bar{E}_{z-} = 0$ due to an excitation by $\bar{H}_{z-}$, as can be also anticipated from the wave equations (19) and (20).

The antenna is approximated by a cylindrical current sheet of surface density J_z of radius "a" and total length "2ℓ." The transform of the current density $J_z(\rho,z)$ is denoted as $\bar{J}_z(\rho,w)$. This current sheet is embedded in a dielectric

cylinder of radius "b" and of relative dielectric constant ϵ_i. The dielectric cylinder is surrounded by an electron plasma with static magnetic field impressed in the direction of the cylinder axis (z-direction). The axial field components are assumed to be in the following form

Region I for $0 \leq \rho \leq a$

$$\bar{E}_{z1} = B_1 J_o(\beta_i \rho) \tag{36}$$

Region II for $a \leq \rho \leq b$

$$\bar{E}_{z2} = B_2 \left[H_o^{(1)}(\beta_i \rho) + R_b H_o^{(2)}(\beta_i \rho) \right] \tag{37}$$

$$\bar{H}_{z2} = A_i J_o(\beta_i \rho) \tag{38}$$

where the expression of $\bar{H}_{z2}$ remains valid also in Region I for $0 \leq \rho \leq a$.

Region III for $b \leq \rho$

$$\bar{E}_{z3} = \sum_j B_{3j} H_o^{(1)}(\beta_j \rho) \tag{39}$$

$$\bar{H}_{z3} = \sum_j A_{3j} H_o^{(1)}(\beta_j \rho) \tag{40}$$

where $\beta_i = \sqrt{\epsilon_1 k_o^2 - w^2}$ and β_j is given by (29), j = + or - , and where $J_n(x)$ is the Bessel function of the first kind of order n.

The amplitudes A_i, B_1, B_2, B_{3j} and A_{3j} are also functions of w. The field components $\bar{E}_{\phi 3}$ and $\bar{H}_{\phi 3}$ are computed after substituting (39) and (40) in (15) and (17). The field components $\bar{E}_{\phi 1}$, $\bar{E}_{\phi 2}$, $\bar{H}_{\phi 1}$ and $\bar{H}_{\phi 2}$ are obtained substituting (38) in (15), (36) and (37) in (17) and by noting that $\epsilon_2 = 0$ and $\epsilon_1 = \epsilon_3 = \epsilon_i$ in the dielectric region. The boundary conditions, $\bar{H}_{\phi 2} - \bar{H}_{\phi 1} = \bar{J}_z$ and continuous $\bar{E}_{z1} = \bar{E}_{z2}$ at $\rho = a$ can be combined to eliminate B_1. After employing the appropriate Wronskian this procedure results in

$$\bar{J}_z = \frac{\delta}{2 J_o(\beta_i a)} \left(-B_2 + B_2 R_b \right) \tag{41}$$

Eliminating A_i from the equations of $\bar{E}_\phi$ and $\bar{H}_z$ continuity at $\rho = b$

$$\sum_j B_{3j} \left[Y_j \frac{H_o^{(1)}(\beta_j b)}{J_o(\beta_i b)} + b_{1j} \frac{H_1^{(1)}(\beta_j b)}{J_1(\beta_i b)} \right] = 0 \tag{42}$$

Continuity of $\bar{H}_\phi$ at $\rho = b$ leads to

$$- \frac{\epsilon_i k_o^2}{\beta_i} B_2 \left[H_1^{(1)}(\beta_i b) + R_b H_1^{(2)}(\beta_i b) \right] + \sum_j B_{3j} b_{2j} H_1^{(1)}(\beta_j b) = 0 \tag{43}$$

Continuity of $\bar{E}_z$ at $\rho = b$ gives

$$- B_2 \left[H_o^{(1)}(\beta_i b) + R_b H_o^{(2)}(\beta_i b) \right] + \sum_j B_{3j} H_o^{(1)}(\beta_j b) = 0 \tag{44}$$

The symbols δ, b_{1j} and b_{2j} are defined by

$$\delta = \frac{4i\epsilon_i k_o^2}{i\omega\mu_o \pi \beta_i^2 a} \tag{45}$$

$$b_{1j} = \frac{\beta_i \beta_j}{i\omega\mu_o D} \left[i\omega\mu_o(\epsilon_1 k_o^2 - w^2) Y_j + \epsilon_2 k_o^2 w \right] \tag{46}$$

$$b_{2j} = \frac{\beta_j}{D} \left[k_o^4(\epsilon_2^2 - \epsilon_1^2) + \epsilon_1 k_o^2 w^2 - i\omega\mu_o \epsilon_2 k_o^2 w Y_j \right] \tag{47}$$

with D defined by (18). The four equations (41) to (44) contain 4 unknown amplitudes B_2, B_2R_2, B_{3+} and B_{3-}, which can be uniquely related to the transformed current density $\bar{J}_z$. The antenna impedance will be specified in Section 3 in terms of the axial electric field $\bar{E}_z$ at the surface of the cylindrical current filament. A straightforward, but lengthy algebraic manipulation shows that $\bar{E}_{z2}$ at $\rho = a$ is related to $\bar{J}_z$ by

$$F(w) = \frac{\bar{E}_{z2}}{\bar{J}_z} = \frac{\alpha_1 \Psi_o - \alpha_2 \Psi_1}{\alpha_1 \alpha_4 - \alpha_2 \alpha_3} \tag{48}$$

where

$$\alpha_1 = a_{1+}a_{2-} - a_{1-}a_{2+} \tag{49}$$

$$\alpha_2 = a_{1+}a_{3-} - a_{1-}a_{3+} \tag{50}$$

$$\alpha_3 = \delta\, J_1(\beta_i b)/J_o(\beta_i a) \tag{51}$$

$$\alpha_4 = \delta\, J_o(\beta_i b)/J_o(\beta_i a) \tag{52}$$

$$\Psi_o = 2i \left[J_o(\beta_i a)\, Y_o(\beta_i b) - Y_o(\beta_i a)\, J_o(\beta_i b) \right] \tag{53}$$

$$\Psi_1 = 2i \left[J_o(\beta_i a)\, Y_1(\beta_i b) - Y_o(\beta_i a)\, J_1(\beta_i b) \right] \tag{54}$$

$$a_{1j} = Y_j \frac{H_o^{(1)}(\beta_j b)}{J_o(\beta_i b)} + b_{1j} \frac{H_1^{(1)}(\beta_j b)}{J_1(\beta_i b)} \tag{55}$$

$$a_{2j} = b_{2j}\, H_1^{(1)}(\beta_j b) \tag{56}$$

$$a_{3j} = (\epsilon_i k_o^2/\beta_i)\, H_o^{(1)}(\beta_j b) \tag{57}$$

and δ, b_{1j}, b_{2j} are defined by (45) to (47). $Y_n(x)$ is the Bessel function of second kind of order n. F(w) of (48) is a complicated function which involves a number of Bessel functions. For uniaxial anisotropy ($\omega_c \to \infty$) when $\epsilon_2 = 0$, (48) can be simplified considerably. It was indicated earlier that $Y_+ \to 0$ and $Y_- \to \infty$ if $\epsilon_2 \to 0$. Applying these conditions and noting that β_+ is given by (32), (48) is changed to

$$F(w) = \frac{\pi a\, \beta_i^2\, J_o(\beta_i a)}{4\,\omega\,\epsilon_o\epsilon_i} \; \frac{\epsilon_3\beta_i\, H_1^{(1)}(\beta_+ b)\, \Psi_o - \epsilon_i\beta_+ H_o^{(1)}(\beta_+ b)\, \Psi_1}{-\epsilon_i\beta_+ H_o^{(1)}(\beta_+ b)\, J_1(\beta_i b) + \epsilon_3\beta_i H_1^{(1)}(\beta_+ b)\, J_o(\beta_i b)} \tag{58}$$

F(w) depends only on the wave number β_+ of the ordinary mode, because the TE field components of the extraordinary mode are not excited with $\epsilon_2 = 0$. For a finite current $I_z = 2\pi a\, J_z$ finite values of the radius 'b' and a vanishingly small radius 'a' of the current filament

$$\frac{\overline{E}_z}{\overline{I}_z} = \frac{\overline{E}_z}{2\pi a\, \overline{J}_z} \approx -\frac{i\beta_i^2}{4\omega\epsilon_o\epsilon_i}\, Y_o(\beta_i a) \tag{59}$$

The field $\overline{E}_z$ is now proportional to $Y_o(\beta_i a)$ which becomes logarithmically infinite as $a \to 0$.

3.0 ANTENNA IMPEDANCE

The driving point impedance of a cylindrical antenna which carries a z-directed current may be computed from the expression

$$Z = - \frac{2\pi a \int E_z J_z dz}{[I(z = 0)]^2} \tag{60}$$

where E_z is computed at the surface of the current filament. Z of (60) is stationary with respect to small changes of the surface current density J_z or of the current I(z) about its correct value[31]. J_z is assumed to be an even function about z = 0. Substituting the Fourier integral representation (7) for $E_z(z)$ and interchanging the order of integrations it follows that

$$Z = - \frac{a}{[I(z=0)]^2} \int_{-\infty}^{\infty} dw\, \bar{E}_z(w) \int_{-\infty}^{\infty} J_z(z) \cos wz\, dz \tag{61}$$

$$= - \frac{a}{[I(z=0)]^2} \int_{-\infty}^{\infty} dw\, F(w) \left[\int_{-\infty}^{\infty} J_z(z) \cos wz\, dz \right]^2$$

where F(w) is defined by (48) or (58). The antenna current density is assumed to be representable by the trial function

$$J_z(z) = A \sin\left[k_A(\ell - |z|)\right] + B \sin\left[k_B(\ell - |z|)\right] \tag{62}$$

Substituting (62) in (61) it follows that

$$Z = \frac{A^2 \gamma_{AA} + 2AB \gamma_{AB} + B^2 \gamma_{BB}}{(AF_A + BF_B)^2} \tag{63}$$

where

$$F_N = \sin k_N \ell \tag{64}$$

$$\gamma_{NM} = - \frac{2}{\pi^2 a} \int_0^{\infty} dw\, F(w)\, g_N(w)\, g_M(w) \tag{65}$$

$$g_N(w) = \int_0^{\ell} \sin\left[k_N(\ell - z)\right] \cos wz\, dz = \frac{k_N}{k_N^2 - w^2} (\cos w\ell - \cos k_N \ell) \tag{66}$$

with N, M = A or B.

The impedance (63) is a function of the amplitude ratio of the two trial functions (A/B). Because of the stationary character of (60), the optimum ratio (A/B) is determined from the condition $dZ/d(A/B) = 0$. This leads to

$$\frac{A}{B} = \frac{\gamma_{BB}F_A - \gamma_{AB}F_B}{\gamma_{AA}F_B - \gamma_{AB}F_A} \tag{67}$$

and

$$Z = \frac{\gamma_{AA}\gamma_{BB} - \gamma_{AB}^2}{\Delta} \tag{68}$$

with

$$\Delta = F_B^2 \gamma_{AA} - 2F_A F_B \gamma_{AB} + F_A^2 \gamma_{BB} \tag{69}$$

The impedance can be also computed for a single term trial function by setting $B = 0$ in (63). This gives

$$Z_s = \frac{\gamma_{AA}}{F_A^2} \tag{70}$$

The impedance formulation (68) which uses the antenna trial functions (62) becomes inaccurate for very short antennas when the two terms of the current distribution are linearly related (i.e. $\sin k_B z = (k_B/k_A) \sin k_A z$ within the computer accuracy). Inaccuracies can be also anticipated for longer antennas if F_A and F_B approach zero simultaneously. In these cases **sine and shifted cosine functions[31] have been used ($\omega > 1.5\ \omega_p$ in Figs. 3 to 5, $\omega \ll \omega_p$ in Fig. 8).**

4.0 IMPEDANCE OF A THIN ANTENNA WITHOUT A DIELECTRIC LAYER

For an antenna without an insulating shell, $b \to a$, Ψ_o of (53) is zero and Ψ_1 of (54) represents a Wronskian. In the limit of $a \to o$ the second term of a_{1j} predominates and it follows that $F(w)$ of (48) can be expressed as

$$F(w) = d_+ \frac{H_o^{(1)}(\beta_- a)}{H_1^{(1)}(\beta_- a)} - d_- \frac{H_o^{(1)}(\beta_+ a)}{H_1^{(1)}(\beta_+ a)} \tag{71}$$

where

$$d_j = \frac{i\omega\mu_o\, b_{1j}}{b_{1+}b_{2-} - b_{1-}b_{2+}} \tag{72}$$

and b_{1j} and b_{2j} are defined by (46) and (47).

4.1 Quasistationary approximations

In the low frequency limit $k_o \to o$, and it will be assumed to be negligible relative to the integration variable w in all of the previous expressions. The wave numbers β_j^2 simplify to $\beta_+^2 = -w^2\,\epsilon_3/\epsilon_1$ and $\beta_-^2 = -w^2$, which makes $d_+ = o$ and $d_- = \omega\mu_o w/(\sqrt{\epsilon_3\epsilon_1}\,k_o^2)$. The antenna impedance is computed from (70) with k_A of the trial functions approaching zero. This results in

$$Z_s = -\frac{2}{\pi^2 a\ell^2}\int_o^\infty dw\, F(w)\left(\frac{1-\cos w\ell}{w^2}\right)^2 \tag{73}$$

Substituting the above values of d_+ and d_- in F(w) of (71) and applying the small argument approximations of the Hankel functions

$$Z_s = -\frac{2i}{\omega\epsilon_o\epsilon_1\pi^2\ell^2}\int_o^\infty \frac{dw}{w^2}(1-\cos w\ell)^2\left[\log w + \log\left(\frac{a}{2}\sqrt{\frac{\epsilon_3}{\epsilon_1}}\right) + C\right] \tag{74}$$

where C = 0.57721 ... is Euler's constant. The integral can be evaluated to give

$$Z_s = \frac{i}{\omega\epsilon_o\epsilon_1\pi\ell}\left[\log\left(\frac{\ell}{a}\right) - 1 + \frac{1}{2}\log\frac{\epsilon_1}{\epsilon_3}\right] \tag{75}$$

Z_s of (75) is the same as the quasi-stationary approximation (63) of Balmain.[15] It will have a resistive component even for a lossless medium if ϵ_1 and ϵ_3 have different signs.

4.2 A short antenna in a uniaxial medium. ($k_o\ell \ll 1$)

In a uniaxial medium $\epsilon_1 = 1$ and $\epsilon_2 = 0$, and the substitution of β_j^2 of (32) and (33) in (72) shows that $d_+ = 0$. F(w) of (71) is simplified to

$$F(w) = \frac{i\omega\mu_o(k_o^2 - w^2)}{k_o^2\,\beta_+}\;\frac{H_o^{(1)}(\beta_+ a)}{H_1^{(1)}(\beta_+ a)} \tag{76}$$

which can be also derived from (58). Substituting (76) in the integral of (70), assuming $k_A = k_o$ and $k_o \ell \ll 1$, and using the small argument approximations of the Hankel functions the real part of the impedance Z_s is computed as

$$R_s = \begin{cases} 20\,(k_o \ell)^2 & \text{for } \omega > \omega_p \\ 60\pi/(k_o \ell) & \text{for } \omega < \omega_p \end{cases} \tag{77}$$

This expression for the resistance (77) has been obtained also by Seshadri.[25] The imaginary part of Z_s is computed as

$$X_s = \frac{i}{\omega \epsilon_o \pi \ell} \left[\log\left(\frac{\ell}{a}\right) - 1 - \frac{1}{2} \log |\epsilon_3| \right] \tag{78}$$

which is valid for short antennas at all frequencies.

The quasistatic approximation (75) gives the same R_s and X_s values as (77) and (78) for $\omega < \omega_p$. This similarity between the quasistatic approximation of the antenna impedance and the impedance of a short antenna in a uniaxial medium has been discussed recently by Mittra.[33]

4.3 The half-wave antenna in free space.

In free space $\beta_+^2 = k_o^2 - w^2$, and applying the small argument approximation of $H_1^{(1)}(x)$, (76) simplifies to

$$F(w) = - \frac{\pi a \omega \mu_o}{2 k_o^2} \left(k_o^2 - w^2 \right) H_o^{(1)} \left(\sqrt{k_o^2 - w^2}\ a \right) \tag{79}$$

For a half-wave antenna $\ell = \lambda/4 = \pi/(2 k_o)$, k_A of the trial functions (62) is set equal to k_o and the antenna impedance is computed from (70). This results in

$$Z = \gamma_{AA} = \frac{\omega \mu_o}{\pi} \int_0^\infty \frac{dw \cos^2\left(\frac{\pi}{2} \frac{w}{k_o}\right)}{k_o^2 - w^2} H_o^{(1)} \left(\sqrt{k_o^2 - w^2}\ a \right) \tag{80}$$

In the limit of $a \to o$ the real part of (80) is given by

$$\text{Re } Z = \frac{\omega\mu_o}{\pi} \int_o^k \frac{dw \cos^2\left(\frac{\pi}{2}\frac{w}{k_o}\right)}{k_o^2 - w^2} \tag{81}$$

which is equal to 73.1 Ohms following equations (36) and (37) of Galejs.[31] The imaginary part of (80) is computed as

$$\text{Im } Z = \frac{\omega\mu_o}{\pi} \int_o^k \frac{dw \cos^2\left(\frac{\pi}{2}\frac{w}{k_o}\right)}{k_o^2} Y_o\left(\sqrt{k_o^2 - w^2}\ a\right)$$

$$+ \frac{2\omega\mu_o}{\pi^2} \int_k^\infty \frac{dw \cos^2\left(\frac{\pi}{2}\frac{w}{k_o}\right)}{w^2 - k_o^2} K_o\left(\sqrt{w^2 - k_o^2}\ a\right) \tag{82}$$

where $K_o(x)$ is the modified Bessel function of second kind and of order zero. In the limit of $a \to o$, small argument approximation of the Bessel functions can be applied to both integrals and (82) simplifies to

$$\text{Im } Z = \frac{\omega\mu_o}{\pi^2} \int_o^\infty \frac{dw \cos^2\left(\frac{\pi}{2}\frac{w}{k_o}\right)}{k_o^2 - w^2} \left[\log\left|1 - \frac{w}{k_o}\right| + \log\left(1 + \frac{w}{k_o}\right)\right] \tag{83}$$

This is equal to (-42.5) Ohms following equation (39) of Galejs.[31] The numerical values of (81) and (83) may be recognized as standard results of antenna theory.

5.0 DISCUSSION OF NUMERICAL RESULTS

5.1 Uniaxial medium

The magnetoionic plasma degenerates into a uniaxial medium with $\epsilon_1 = 1$ and $\epsilon_2 = 0$ in the presence of strong magnetic fields ($\Omega_c = \omega_c/\omega_p \to \infty$). For such a medium the antenna impedance is shown in Fig. 1, where the left-hand scale of the resistance applies for $\omega < \omega_p$ and the right-hand scale for $\omega > \omega_p$. The calculations are made for antennas of length $\lambda/20$ and $\lambda/10$ (indexes 1 and 2) and for very small ($b - a < 10^{-4}\ \lambda$) and for larger ($b - a = \lambda/100$) radii of an insulating layer around the antenna (indexes p and i).

The antenna radius a and length 2ℓ are such that $\Omega = 2 \log (2\ell/a) = 8$. The medium has slight losses with an average collision frequency $\nu = 0.001\ \omega_p$. The resistance is nearly constant for $\omega > \omega_p$, increases suddenly near $\omega = \omega_p$ and reaches its maximal value for $\omega < \omega_p$. The resistance decreases gradually for lower values of ω or higher values of ω_p. The resistance is proportional to ℓ^2 for $\omega > \omega_p$ and is inversely proportional to ℓ for $\omega < \omega_p$. The reactance is **capacitive** for the frequency range indicated in Fig. 2, and for a lossless plasma it becomes logarithmically infinite at $\omega = \omega_p$. The reactance is decreasing for higher values of ω_p, and it will become inductive for sufficiently large values of ω_p. The same general impedance behavior is also observed from the approximate impedance expression (77) and (78) which are indicated by thin lines in Fig. 1. An insulating layer around the antenna of $b - a = \lambda/100$ (index i in Fig. 1) has little effect for frequencies $\omega > \omega_p$, but it tends to decrease the resistance and to make the reactance more capacative for $\omega < \omega_p$.

5.2 Antenna resistance in a magnetoionic medium.

The antenna impedance can be calculated from (70) for an assumed sinusoidal current distribution which becomes triangular for short antennas. The real part of the computed impedance is shown in Fig. 2 for an antenna of length $\ell = c/\omega_p$ ($\ell = \lambda/(2\pi)$ at $\omega = \omega_p$). The antenna has a finite radius ($\Omega = 12.5$) and the surrounding medium has also slight losses ($\nu/\omega_p = 10^{-3}$). The calculations are made for a plasma of $\Omega_c = \omega_c/\omega_p = 0.5$ and 1.5. The resistance has a large but finite peak at the upper hybrid resonance frequency $\omega_u = \sqrt{\omega_c^2 + \omega_p^2}$ which is indicated in Fig. 2 as $\Omega_u = \omega_u/\omega_p$. The radiation resistance becomes large for small and large values of ω/ω_p. The radiation resistance of a current filament with an assumed triangular current distribution has been computed recently by Seshadri[22] for a lossless medium. These data are indicated by thin lines in Fig. 2, and they agree with the present computation in particular for the lower frequencies. However for a lossless medium and $\omega_c < \omega_p \sqrt{2}$ the resistance is

equal to zero in the frequency range $\omega_c < \omega < \omega_1$, where $\omega_1 = 0.5\ (-\omega_c + \sqrt{\omega_c^2 + 4\omega_p^2}\ )$. The resonance peak observed for $\omega_c = 1.5\ \omega_p$ at $\omega = \omega_p$ is higher for a lossless medium and the two sets of calculations differ significantly for higher frequencies where the triangular current distribution becomes inaccurate. However, the assumed sinusoidal current gives a high resistance for $\ell \approx \lambda/2$ (or near $\omega = 3\omega_p$).

5.3 Antenna impedance

The antenna impedance is computed next using a two term trial function (62) with $k_A = k_B/2 = k_o$. Such trial functions can be shown to be adequate for impedance calculations in free space if the antenna length is not near a multiple of $\lambda/2$, and they will also indicate the frequency ranges where the electrical antenna length becomes large in a magnetoionic medium and where further resonances may be expected. The calculations of Fig. 3 are made for the normalized gyro frequency $\Omega_c = \omega_c/\omega_p = 0.5$ and an additional resonance is observed for frequencies ω which are somewhat less than ω_c , if the insulating layer is of negligible thickness (b -a). Increasing losses($\nu/\omega_p = 10^{-2}$) will decrease this resonance peak and the losses also increase the resistance in the frequency range $\omega_c < \omega < \omega_1$, where the resistance is zero for a lossless plasma. An insulating layer (or ion sheath) of a thickness b -a = $\lambda/100$ shifts the resonance to frequencies $\omega > \omega_c$. Also it makes the reactance more capacitive for $\omega < \omega_u$ and slightly more inductive for $\omega > \omega_u$. The antenna resistance is decreased for $\omega \ll \omega_p$. A similar impedance behavior is also seen in Fig. 4 for $\Omega_c = 1.5$. The additional resonance peak is observed for $\omega < \omega_c$, if the insulating layer is thin, and the resonance peak is shifted closer to the frequency ω_c for increased thickness of the insulating layers.

The presence of the resonance peak in the vicinity of ω_c indicates that the antenna becomes electrically long as ω approaches ω_c. Under these conditions ϵ_1 approaches infinity and the resonance can be explained possibly by a propagation coefficient of the current distribution which is proportional to the $\sqrt{\epsilon_1}$, following the suggestion of Ament et al.[30] Further calculations are therefore made using the trial functions $k_A = k_s$, $k_B = 2\ k_s$, where $k_s = \sqrt{\mathrm{Re}\ \epsilon_1}\ k_o$. The

impedance curves shown in Fig. 5 exclude the frequency range $\omega_c < \omega < \omega_u$, where Re ϵ_1 is negative, because the present computer program is intended for real coefficients k_A and k_B only in (64) and (66). The resonance peaks are higher than in Fig. 3 and 4, and there are also further resonances in the immediate vicinity of ω_c, which could not be shown in the frequency scale used in Fig. 5. The impedance computed from two-term trial functions is also nearly the same as the computations which are based only on $k_A = k_s$ from Eq. (70). The ratio of the trial function amplitudes A/B is computed from (67). The magnitude of A/B is of the order 5 to 10, and this shows that the predominant term of the antenna current representation has a wave number $k_A = k_s$. Further calculations have been made using $k_A = k_s$ and $k_B = k_s/2$. Again the magnitude of A/B is larger than unity and the impedance is nearly the same as for $k_B = 2\ k_s$ shown in Fig. 5. This suggests that the wave number k_s may be good first order estimate of the current distribution along the antenna, if the thickness of the insulating cover is negligible. This hypothesis will be checked by plotting several variationally computed current distributions and by comparing them with a single sine wave having a wave number k_s.

The calculations of Figs. 6a and b are made for frequencies near the resonance peak $\omega < \omega_c$. For small values of (b -a) the two sets of calculations using $k_A = k_s$ and $k_B = 2\ k_s$ (dashed curve) or $k_B = 0.5\ k_s$ (dashed and dotted curve) give essentially similar current distributions. The calculations using free space wave number $k_A = k_o$ and $k_B = 2\ k_o$, indicated by solid curves, approximate the other current distributions more closely in Fig. 7b, because ϵ_1 of (4) is smaller in magnitude for larger values of ω_c, and k_s differs less from k_o for ω_c large. The thin line denotes a simple sine wave with a wave number k_s, and it lies below the other curves. This indicates that the wave number of the current distribution is somewhat larger than k_s in Figs. 7a and 7b.

For an insulating layer of thickness (b-a) = $\lambda/100$ the current distribution is quite different. It is nearly triangular for $\omega_c/\omega_p = 0.5$ and it has a relatively low peak for $\omega_c/\omega_p = 1.5$. The insulating layer tends to make the antenna electrically shorter for frequencies near ω_c, and the simple approximation of the wave number of the current distribution by k_s that may be justified for antennas in direct contact with a surrounding plasma, definitely will be in error in the presence of an insulating layer or an ion sheath.

Further calculations are shown in Figs. 6c and d for antennas of negligibly thin insulating layers and for frequencies ω in the immediate vicinity of ω_c. The thin line which is sine wave with a wave number k_s, approximates the current distributions computed with $k_A = k_s$ and $k_B = 2\ k_A$ or $k_B = k_A/2$. The agreement is particularly close for $\omega_c/\omega_p = 0.5$, but even for $\omega_c/\omega_p = 1.5$ the wave number k_s gives a first order estimate for the propagation coefficient of the current distribution. This propagation coefficient k_s should not be identified as a wave number of surface waves which do not exist with a lossless plasma for frequencies ω above the lowest of ω_p or ω_c following Seshadri.[34] Obviously the surface waves cannot explain the resonances shown in Figs. 3 and 5b, which occur in the frequency range $\omega_p < \omega < \omega_c$. Also, the approximation of the propagation coefficient by k_s will not apply to antennas insulated from the surrounding plasma.

It has been suggested that the wave number of plane waves which propagate along the antenna may characterize the current distribution on the antenna.[29] One of the wave numbers given by (31) which is proportional to $\sqrt{\epsilon_1 - \epsilon_2}$ becomes very large as ω approaches ω_c, it is nearly real for $\omega < \omega_c$ and it becomes imaginary for $\omega > \omega_c$. However for $\omega \approx \omega_c$ its magnitude is by a factor of $\sqrt{2}$ larger than the magnitude of k_s. Such a current distribution was not observed in the curves of Figs. 6c and d, although the trial functions used in the impedance computation ($k_A = k_s$, $k_B = 2\ k_s$) are general enough to account for it.

5.4 Comparisons with other impedance calculations

The present calculations are compared in Fig. 7 with the result shown in Figs. 14 and 15 by Ament et al.[27] for $\omega > \omega_p$. Ament et al.[27] assume a sinusoidal current distribution with a wave number $\sqrt{\epsilon_3}\ k_o$. The two sets of resistance data are in reasonable agreement but the differences in the reactance curves can probably be explained by differences of the trial functions, which should have the most pronounced effects near the resonance length of the antennas.

The present calculations are further compared with the quasi-stationary approximation (75) using the plasma parameters shown as cases 2 and 3 in table 4 of Ament et al.[30] The quasi-stationary approximation, indicated by thin lines, follows the trend of the more accurate calculations and it shows a somewhat lower antenna resistance. The capacative reactance of the two calculations differ by a factor of nearly two in the case B. The data shown in Fig. 8 differ considerably from the calculations of Ament et al.[30] Their resistance values are in most cases lower by a factor of approximately 100. Furthermore the reactance is inductive and is three times larger than the magnitude shown in case A, and it differs by several orders of magnitude for most of the points of case B. The results of Ament et al[30] are not shown in Fig. 8.

The current calculations are compared further with the quasi-stationary approximations and with the computation by Staras[28] in Fig. 9. The quasi-stationary approximations agree closely with the more accurate calculations for long thin antennas. However for short antennas (antenna of a smaller ℓ/a ratio) the quasi-stationary approximation indicates a resonance. The antenna can be shown to remain electrically short in the vicinity of this resonance and therefore the accuracy of the quasi-stationary formula should be questioned. (This apparent resonance is due solely to the decrease of the ℓ/a ratio in Eq. (75) but the quasi-stationary approximations are known to become inaccurate for antennas of decreasing ℓ/a). The resistance points listed by Staras[28] show the

same trend as the present calculations, but the reactance is of different signs. It may be noted that Staras[28] uses a volumetric current distribution which does not correspond directly to a fixed antenna surface as used in the present investigation.

The results of Brandstatter and Penico[29] were briefly discussed in Section 1. These impedance figures are of such magnitude that a closer comparison with the results of the present calculations does not appear warranted.

5.5 Limitations of the analysis

Only antennas of $\ell < 0.5\lambda$ are investigated in the present paper. For such antenna lengths the triangular current distributions of very short antennas are inadequate, but it is not necessary to apply the theory of long antennas. In this intermediate range of antenna lengths variational impedance formulations have been successfully applied for antennas in free space and also in stratified dielectric layers.[32]

The impedance formulas are stationary only with respect to small changes ΔJ_z about the correct current density J_{cz}, and large changes of the impedance can be anticipated if ΔJ_z differs significantly from J_{cz}. The converse of this property can be readily utilized. If the impedances computed using different trial functions remain nearly constant, it may be concluded that the assumed trial functions are general enough and that the resulting current distributions do not depart significantly from the true current density J_{cz}, at least for purposes of calculating the impedance, and that the resulting impedance is correct. The constancy of the impedance can be verified by comparing Figs. 3 and 4 with Fig. 5. The impedances are practically the same, except for ω near ω_c where the antennas become electrically long and the trial functions with $k_A = k_B/2 = k_0$ of Fig. 3 and 4 cannot produce a sufficiently oscillatory distribution. The current distributions of the variational impedance calculations differ by approximately 10 percent in Figs. 6a and b. In the present method it is not possible to select the best one among the several approximations, although an auxiliary condition

of $E_z = 0$ could be used for fields on a perfectly conducting antenna.

The purpose of the present paper was to show that the impedance of the linear antenna can be computed in magnetoionic media with current distributions that are more accurate than the usually assumed triangular or half wave sinusoidal distributions, and to emphasize the presence of multiple antenna resonance as ω approaches ω_c. The current distributions are obviously approximate, but the computed antenna impedances are considered reliable within the accuracy of the numerical plots, except in the vicinity of the frequencies where $\omega \tilde{=} \omega_c$. Here the antenna is electrically long and the variational impedance formulation will become inaccurate even in free space for reasons mentioned in the concluding paragraph of Section 3.

5.6 Summary of Conclusions

This paper has presented impedance calculations over the complete frequency range. For a uniaxial medium approximate closed form expressions compare with the more accurate numerical calculations. There is good agreement with the antenna resistance as computed by Seshadri[22] over the frequency range where his triangular current distributions is justified, but further resonances are observed for frequencies in the vicinity of the gyro frequency. By examining a number of trial functions for the current distributions of the antenna it was deduced that $\sqrt{\epsilon_1}\, k_o$ represents a first order estimate of the wave number for the current distributions along the antenna if the antenna insulation is of a negligible thickness. This estimate applies both above and below the plasma frequency but it is not valid for insulated antennas. For frequencies exceeding the plasma frequency, the calculations compare with the work of Ament et al.[27], and for frequencies much lower than the plasma frequency there is an indication of the validity of quasi-static calculations. The resistance values listed by Staras[28] can be compared with the present work. However he indicates an inductive reactance whereas the present calculations give a capacitive reactance for the same antenna parameters. There is a definite disagreement between the present

calculations and the recent work of Brandstatter andPenico[29] and Ament et al.[30] for low frequencies.

6.0 ACKNOWLEDGMENTS

Appreciation is expressed to D. A. Breault for computer programming.

The work reported here was supported in part by contract AF 19(628)-2410 with the Office of Aerospace Research, United States Air Force.

REFERENCES

1) Abraham, L.G., "Extensions of the magnetoionic theory for radio-wave propagation in the ionosphere including antenna radiation and plane wave scattering," School of Electrical Engineering, Cornell University, Tech. Report No. 13, 1953.

2) Chow, Y., "A note on radiation in a gyroelectric-magnetic medium - an extension of Bunkin's calculation," IRE Trans. on Antennas and Propagation, Vol. AP-10 pp. 464-469, July 1962.

3) Kuehl, H. H., "Radiation from an electric dipole in an anisotropic cold plasma" Phys. of Fluids, Vol. 5, pp.1095-1103, September 1962.

4) Hodara, H. and G.I. Cohn, "Radiation from a gyro-plasma coated magnetic line source," IRE Trans. on Antennas and Propagation, Vol. AP-10, pp.581-593, September, 1962.

5) Hodara, H., "Radiation from a gyro-plasma sheathed aperture," IEEE Trans. on Antennas and Propagation, Vol. AP-11, pp.2-12; January, 1963.

6) Clemmow, P.C., "The theory of electromagnetic waves in a simple anisotropic medium," Proc. IEE (London), Vol. 110, pp.101-106; January 1963.

7) Clemmow, P.C., "On the theory of radiation from a source in a magnetoionic medium," in Electromagnetic Waves, edited by E. C. Jordan, Pergamon Press, New York, N.Y., Part I, pp.461-475, 1963.

8) Arbel, E. and Felsen, L.B., "Theory of radiation from sources in anisotropic media," in Electromagnetic Waves, edited by E. C. Jordan, Pergamon Press, New York, N.Y., Part I, pp.391-459, 1963.

9) Wu, C.P., "Radiation from dipoles in a magnetoionic medium," IEEE Trans. on Antennas and Propagation, Vol. AP-11, pp.681-689, November 1963.

10) Mittra, R. and G. A. Deschamps, "Field solutions for a dipole in an anisotropic medium," in Electromagnetic Waves, edited by E. C. Jordan, Pergamon Press, New York, N.Y., Part I, pp. 495-512; 1963.

11) Wait, J. R., "Theory of radiation from sources immersed in anisotropic media" Journal of Research, NBS, Vol. 68B, No. 3, pp.119-136; July-Sept. 1964.

12) Deschamps, G.A. and O. Kesler, "Radiation field of an arbitrary antenna in a magnetoplasma," IEEE Transactions on Antennas and Propagation, Vol. AP-12, pp.783-785; November, 1964.

13) Bramley, E. N., "The admittance of a short cylindrical dipole in the ionosphere" Planet. Space Sci., Vol. 9, pp.445-454; August 1962.

14) Kaiser, T. R., "The admittance of an electric dipole in a magnetoionic environment," Planet. Space Sci., Vol. 9, pp.639-657; October, 1962.

15) Balmain, K.G., "The impedance of a short dipole antenna in a magnetoplasma" IEEE Transactions on Antennas and Propagation, Vol. AP-12, pp.605-617; September, 1964.

References (continued)

16) Kogelnik, H., "On electromagnetic radiation in magnetoionic media," NBS, Journal of Research, Vol. 64D, No.5, pp.515-522; September-October, 1960.

17) Kogelnik, H., "The radiation resistance of an elementary dipole in anisotropic plasma," Proc. 4th International Conf. on Ionization Phenomenon in Gases, North Holland Publishing Co., 1960.

18) Kogelnik, H. and H. Motz, "Electromagnetic radiation from sources embedded in an infinite anisotropic medium and the significance of the Poynting vector," in Electromagnetic Waves, edited by E. C. Jordan, Pergamon Press, New York, N.Y., Part I, pp.477-493; 1963.

19) Weil, H. and D. Walsh, "Radiation resistance of an electric dipole in a magnetoionic medium," IEEE Transactions on Antennas and Propagation, Vol. AP-12, pp.297-304; May, 1964.

20) Weil, H. and D. Walsh, "Radiation resistance of an elementary loop antenna in a magnetoionic medium," IEEE Transactions on Antennas and Propagation, Vol. G-AP-13, pp.21-27; January, 1965.

21) Motz, H., "On electromagnetic radiation from a magnetic dipole with arbitrary orientation embedded in a lossless magnetoionic medium," J. of Res., NBS/USNC-URSI, Vol. 69D, No. 5, pp.671-679; May, 1965.

22) Seshadri, S. R., "Radiation resistance of elementary electric current sources in a magnetoionic medium," Proc. IEE, Vol. 112, No. 10, pp.1856-1868, October 1965.

23) Seshadri, S.R., "Radiation from a current strip in a uniaxially anisotropic plasma medium," Can. J. of Physics, Vol. 44, 1966.

24) Seshadri, S.R. and M. S. Tuan, "Radiation resistance of a circular current filament in a magnetoionic medium," Proc. IEE, Vol. 112, No. 12, Dec. 1965.

25) Seshadri, S.R., "Radiation resistance of a linear current filament in a simple anisotropic medium," IEEE Transactions on Antennas and Propagation, Vol. AP-13, No. 5, pp.819-820; September, 1965.

26) Seshadri, S.R., "Effect of insulation on the radiation resistance of an electric dipole in a simple anisotropic medium," Proc. IEE, Vol. 113 1966

27) Ament, W. S., J.C. Katzı , M. Katzin, and B.Y.C. Koo, "Impedance of a cylindrical dipole having a sinusoidal current distribution in homogeneous anisotropic ionosphere," Journal of Research NBS/USNC-URSI, Radio Science, Vol. 68D, No. 4, pp.379-405; April, 1964.

28) Staras, H., "The impedance of an electric dipole in a magnetoionic medium" IEEE Trans. on Antennas and Propagation, Vol. AP-12, pp.695-702, Nov. 1964.

References (continued)

29) Brandstatter, J. J. and A. J. Penico, "A study of the impedance of a cylindrical dipole in an anisotropic plasma," Final Report, Project PMU-3417, Stanford Research Institute, Menlo Park, California, November, 1964.

30) Ament, W. S., M. Katzin, J. R. McLaughlin and W. W. Zachary, "Satellite antenna radiation properties at VLF in the ionosphere." Final Report on Contract Nonr-4250(00)(X), Electromagnetic Research Corporation, College Park, Md., April, 1965.

31) Galejs, J., "Driving point impedance of linear antenna in the presence of a stratified dielectric," IEEE Transactions on Antennas and Propagation, Vol. AP-13, No. 4, pp.725-737; September 1965.

32) Kamke, E., "Differential Gleichungen," Chelsea Publishing Company, New York, N.Y.; 1948.

33) Mittra, R., "Radiation Resistance of Antennas in Anisotropic Media," Electronics Letters, Vol. 1, No. 9, pp.258-259; November, 1965.

34) Seshadri, S. R., "Guided waves on a perfectly conducting infinite cylinder in a magnetoionic medium," Proc. IEE, Vol. 112, No. 8, pp.1497-1500; August, 1965.

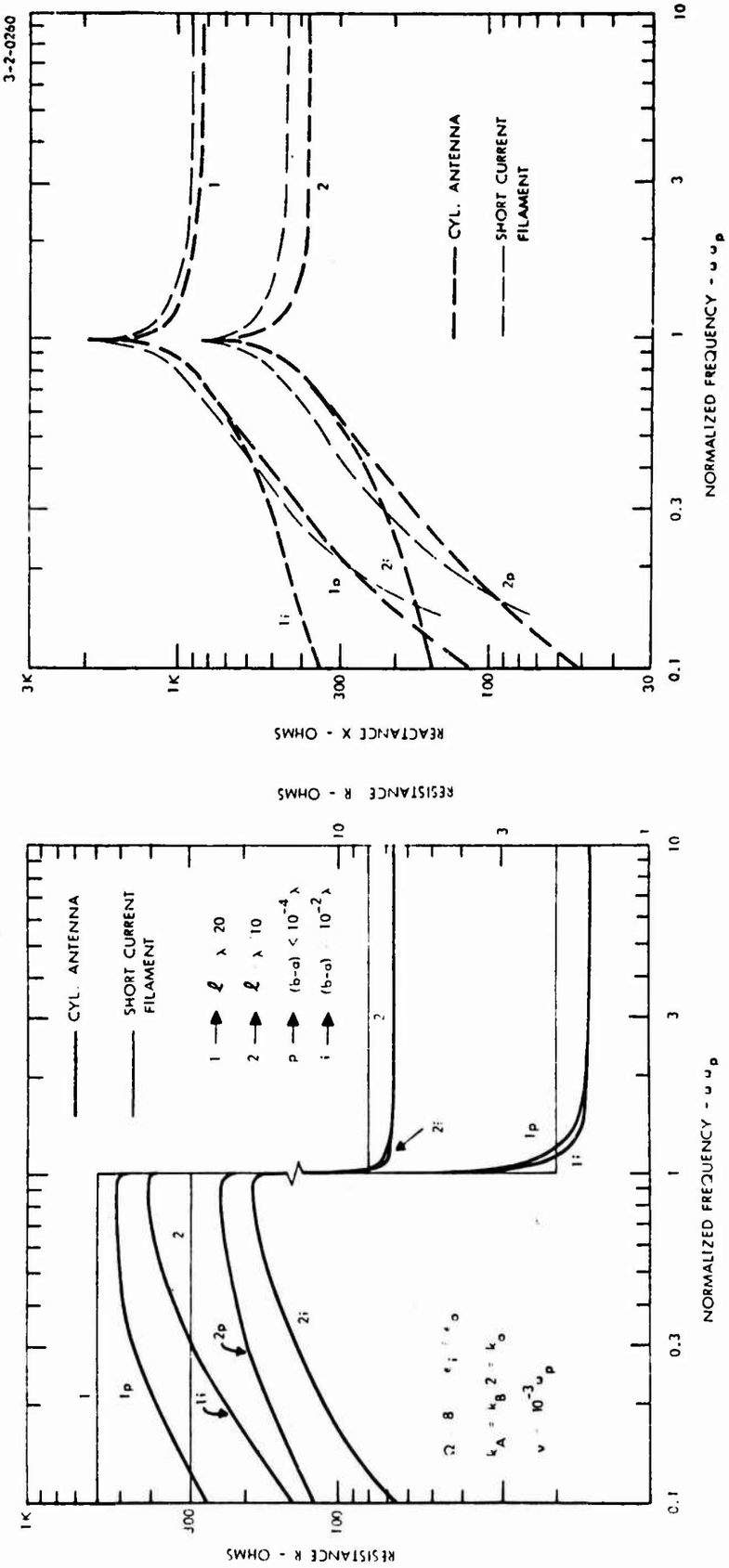

Figure 1. Impedance of a Short Antenna in a Uniaxial Medium.

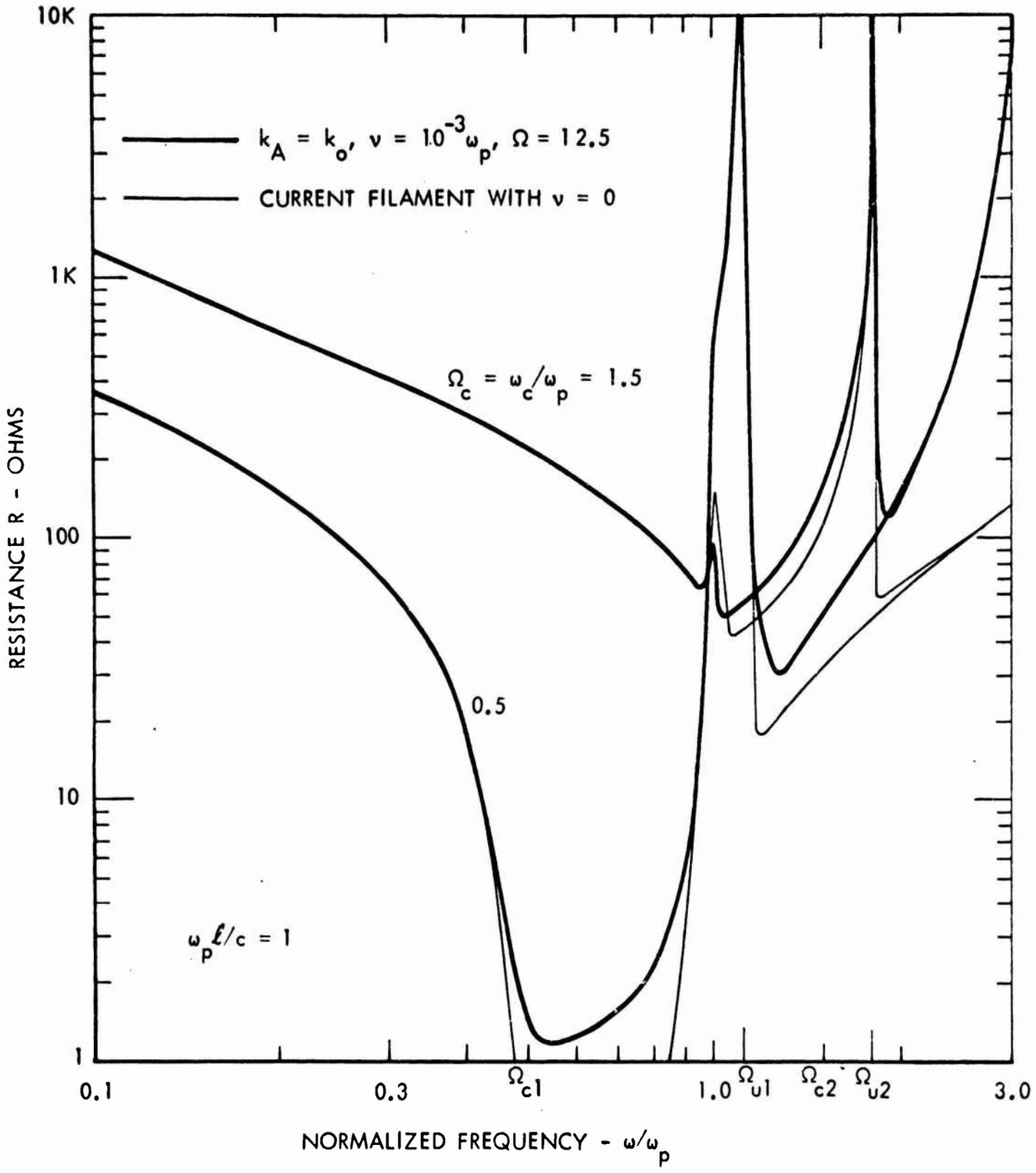

Figure 2. Antenna Resistance for Sinusodail and Triangular Current Distributions.

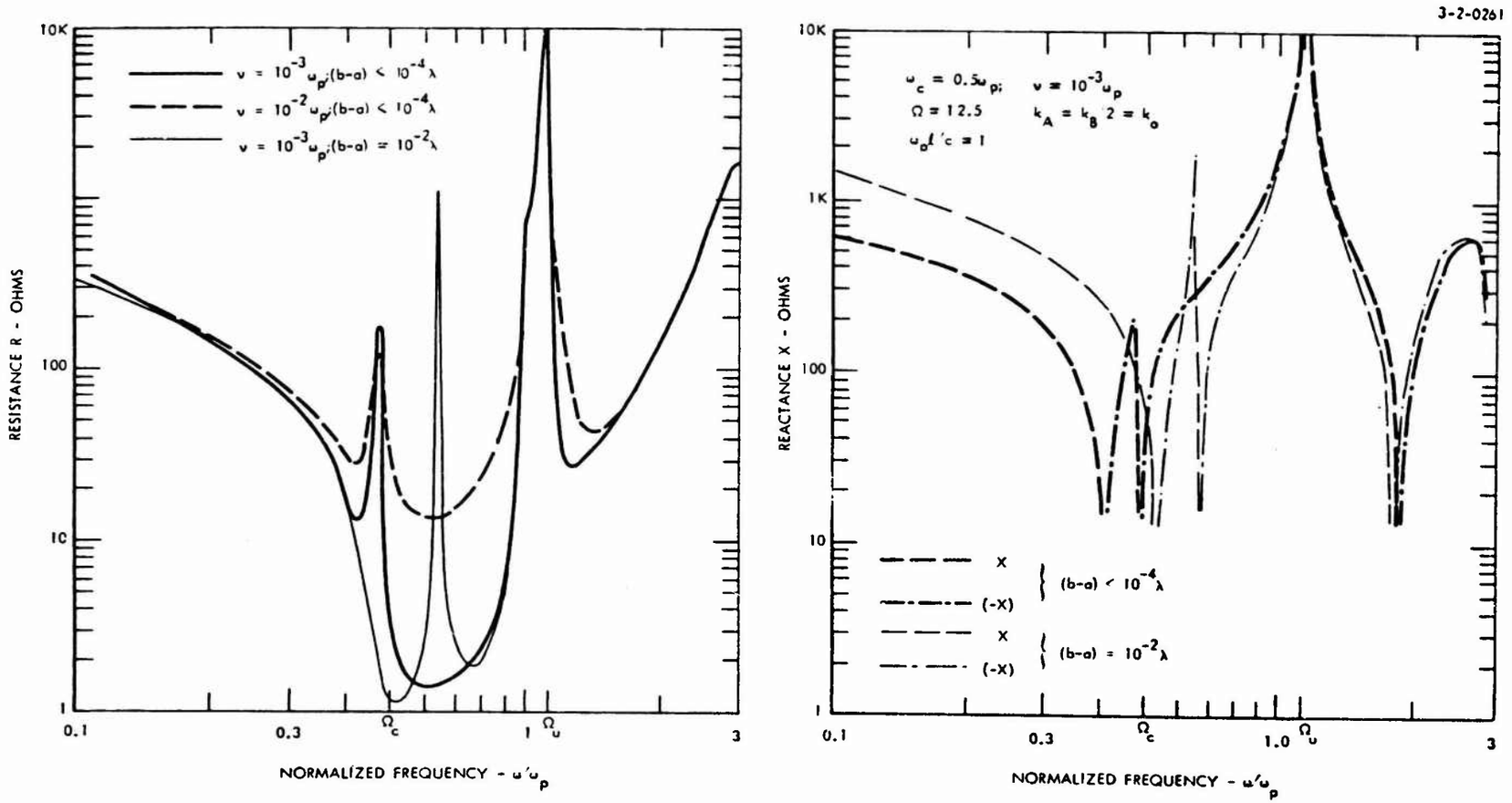

Figure 3. Antenna Impedance Using the Trial Functions $k_A = k_B/2 = k_o$; $\Omega_c = \omega_c/\omega_p = 0.5$.

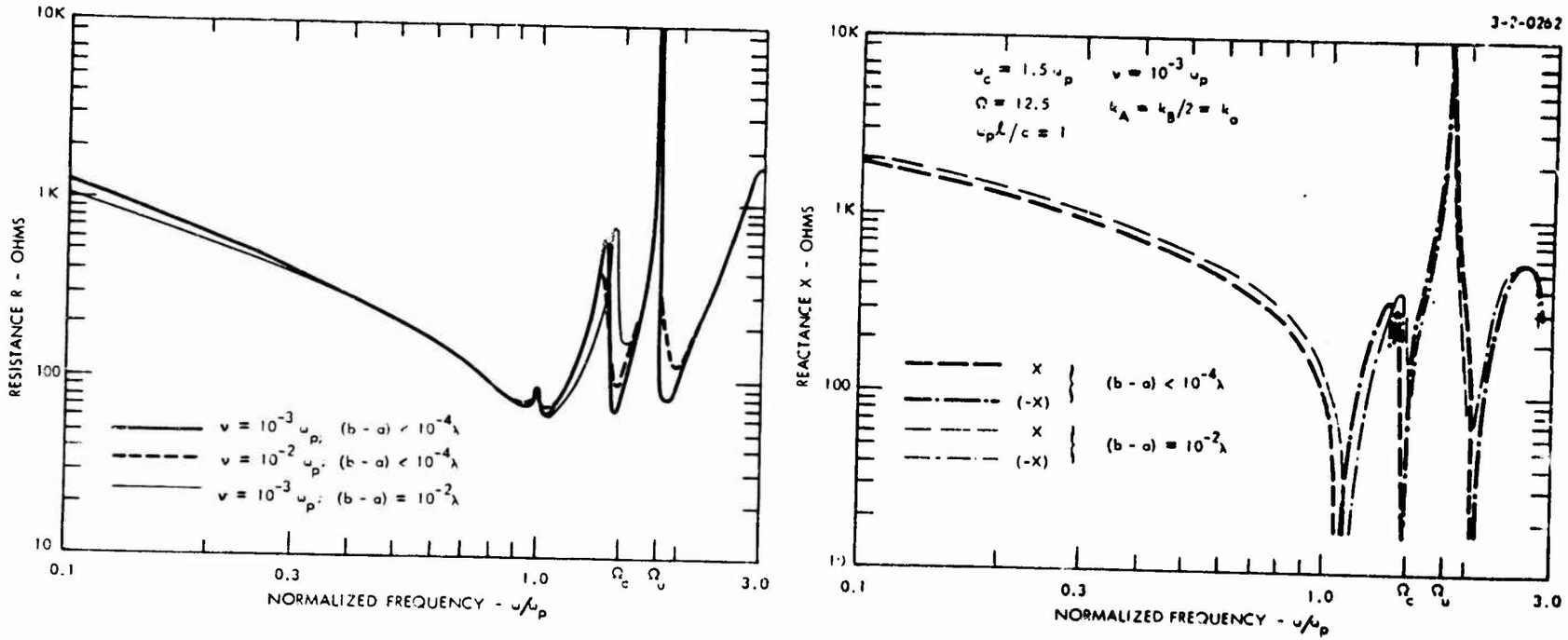

Figure 4. Antenna Impedance Using the Trial Functions $k_A = k_B/2 = k_o$; $\Omega_c = \omega_c/\omega_p = 1.5$.

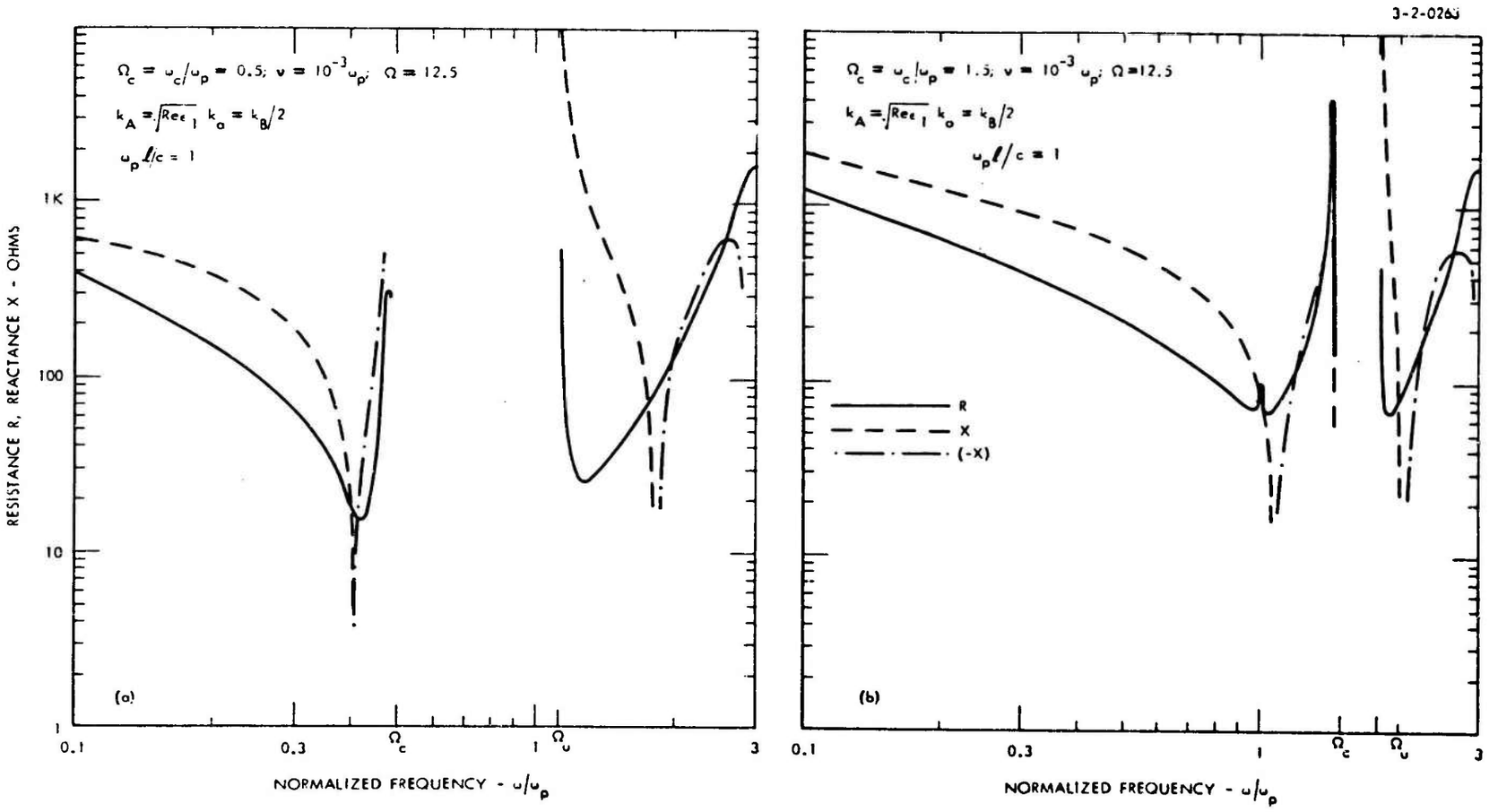

Figure 5. Antenna Impedance Using the Trial Functions $k_A = k_B/2 = \sqrt{Re\epsilon}_1\, k_o$.

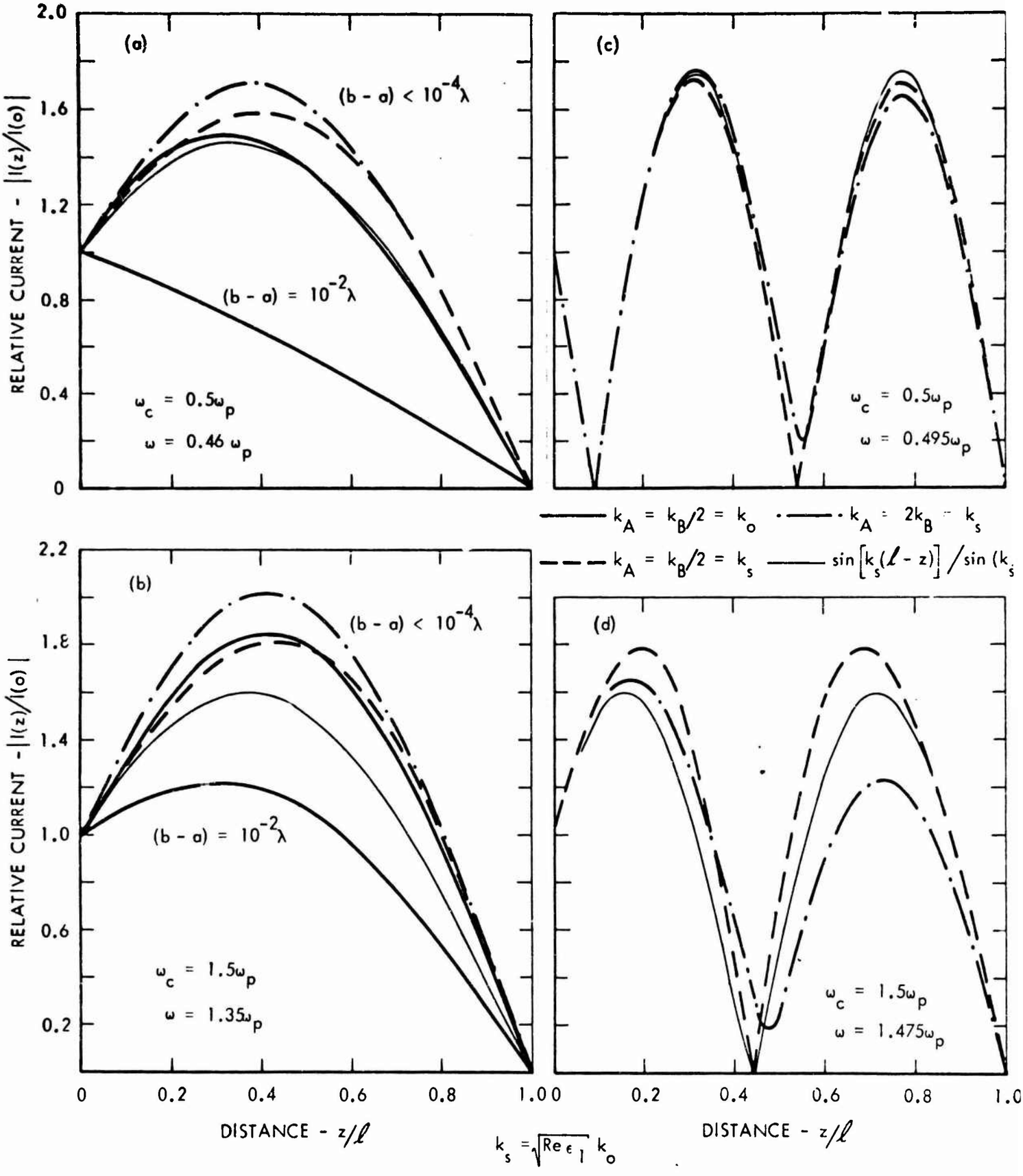

Figure 6. Variational Approximations to the Current Distributions.

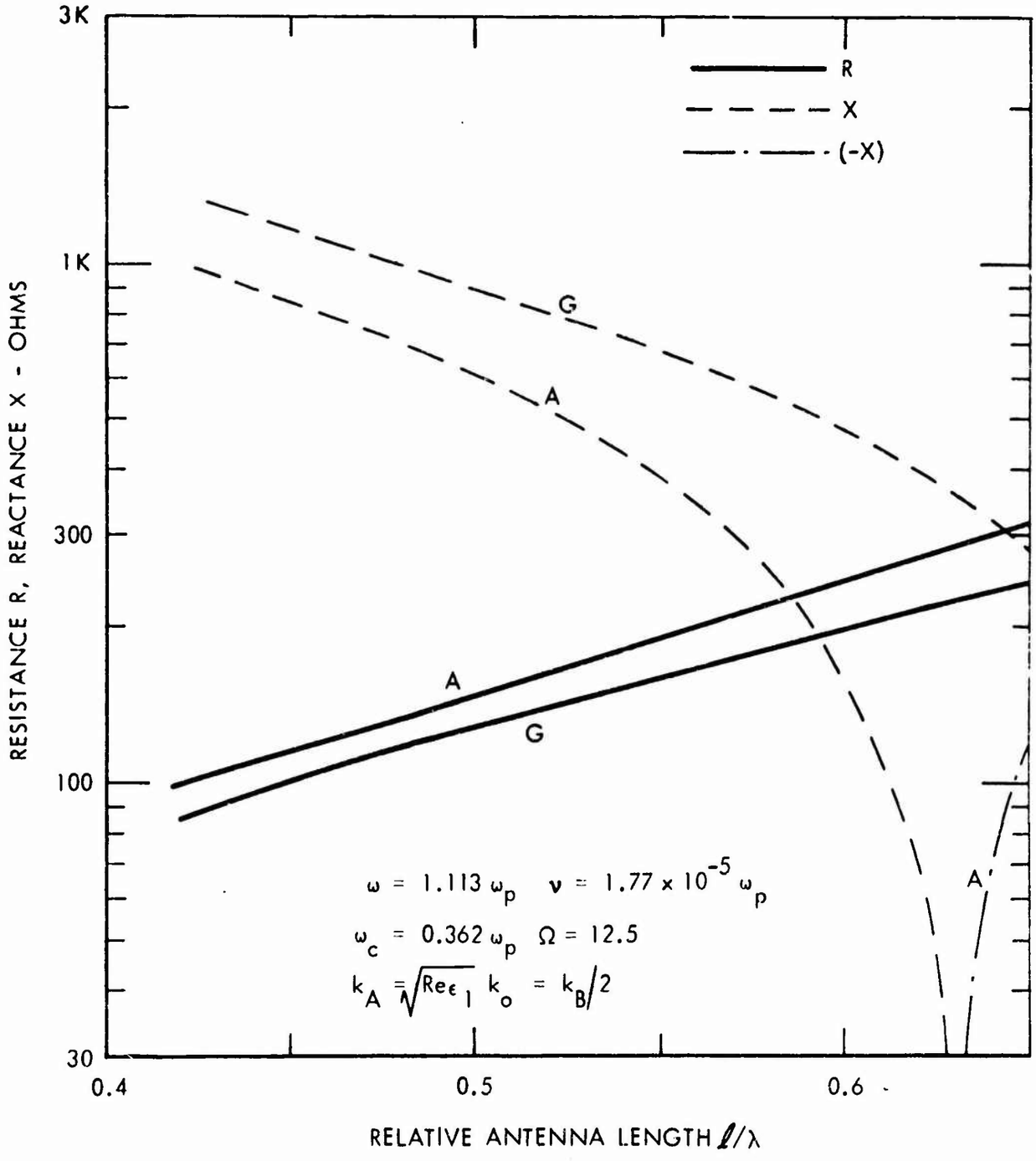

Figure 7. Antenna Impedance for $\omega > \omega_p$. Present formulation (G) and calculations by Amentetal (A).

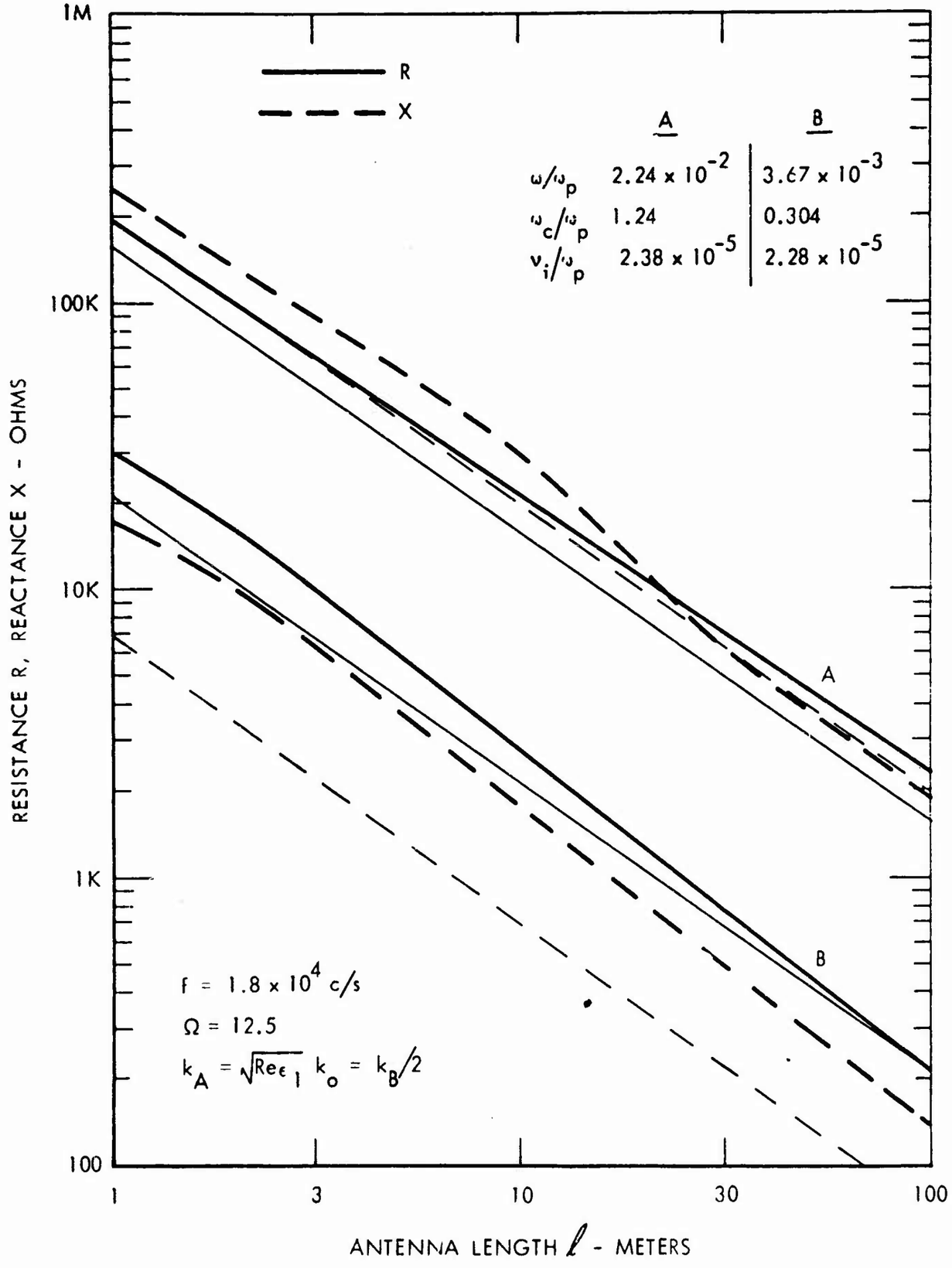

Figure 8. Antenna Impedance for $\omega << \omega_p$. Comparison with the quasistatic approximation (thin lines).

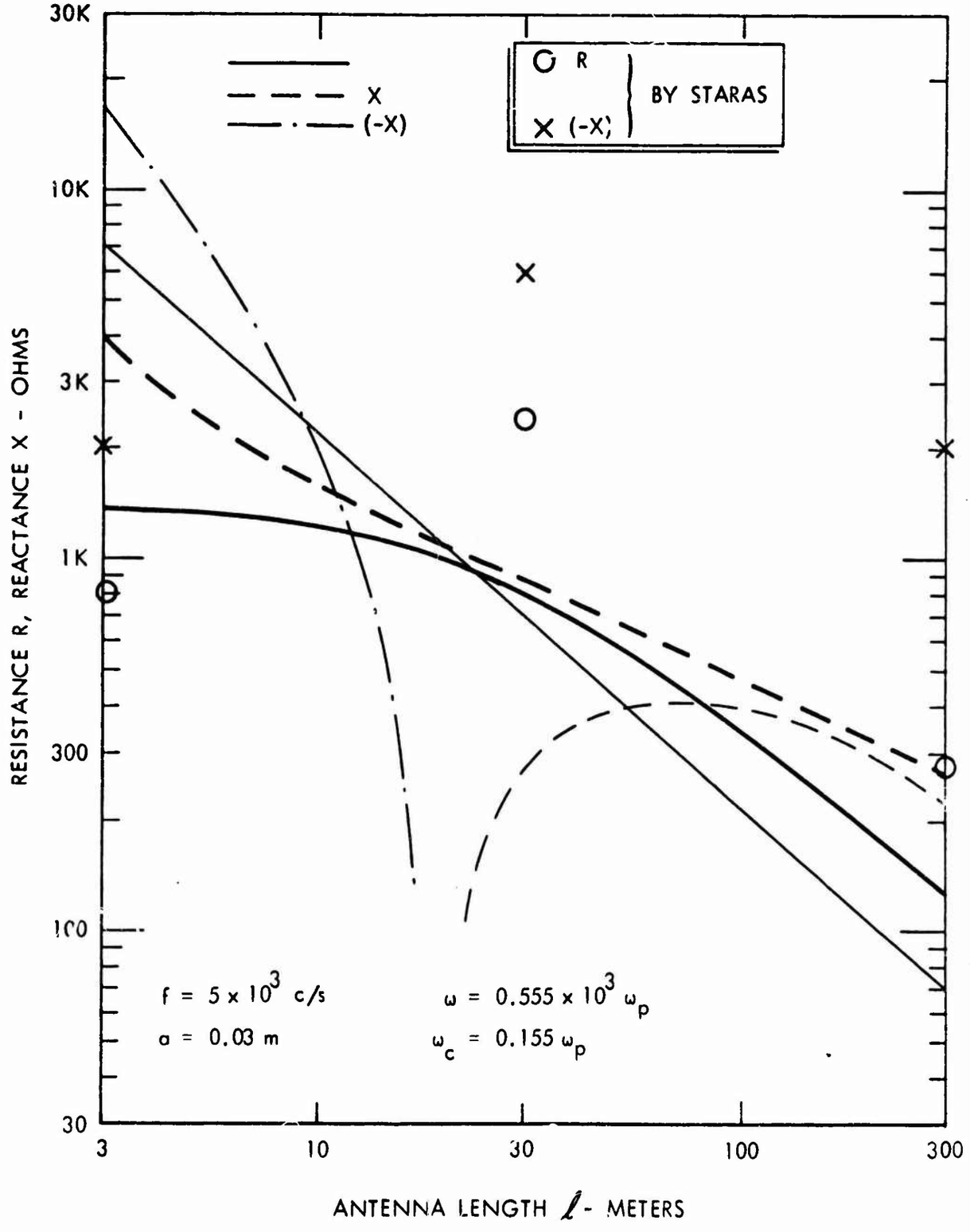

Figure 9. Antenna Impedance for $\omega << \omega_p$. Comparison with the quasistatic approximation (thin line) and with computations by Staras.

Unclassified
Security Classification

DOCUMENT CONTROL DATA - R&D

(Security classification of title, body of abstract and indexing annotation must be entered when the overall report is classified)

1. ORIGINATING ACTIVITY *(Corporate author)*
Applied Research Lab., Sylvania Electronic Systems
A Division of Sylvania Electric Products, Inc.
40 Sylvan Road, Waltham, Massachusetts 02154

2a. REPORT SECURITY CLASSIFICATION
Unclassified

2b. GROUP
N/A

3. REPORT TITLE
Impedance Of A Finite Insulated Cylindrical Antenna In A Cold Plasma With A Longitudinal Magnetic Field

4. DESCRIPTIVE NOTES *(Type of report and inclusive dates)*
Scientific Report No. 2 - Interim

5. AUTHOR(S) *(Last name, first name, initial)*
Galejs, J.

6. REPORT DATE	7a. TOTAL NO. OF PAGES	7b. NO. OF REFS
25 July 1966	40	34

8a. CONTRACT OR GRANT NO.	9a. ORIGINATOR'S REPORT NUMBER(S)
AF19(628)-5718	RR-491
b. PROJECT NO. and Task No. 4642,02	S-5158-2
DoD element 62405304	9b. OTHER REPORT NO(S) *(Any other numbers that may be assigned this report)* AFCRL-66-551
d. DoD subelement 674642	

10. AVAILABILITY/LIMITATION NOTICES
Distribution of this document is unlimited.

11 SUPPLEMENTARY NOTES	12 SPONSORING MILITARY ACTIVITY
NONE	HQ. AFCRL, OAR (CRD) United States Air Force L. G. Hanscom Field, Bedford, Mass.

13. ABSTRACT A variational formulation is developed for the impedance of a finite cylindrical antenna embedded in a dielectric cylinder, which is surrounded by a magnetoionic medium (cold electron plasma) with the static magnetic field impressed in a direction parallel to the antenna axis. Closed form expressions are obtained in the limit of low frequencies, and for short antennas in a uniaxial medium. The impedance of a short antenna is nearly the same as for an assumed triangular current distribution, except that further resonances are observed in the vicinity of the gyro frequency, where the antenna becomes electrically long. These resonances may be shifted to frequencies exceeding the gyro frequency in the presence of an insulating layer around the antenna. For very thin insulating layers the wave number of the variationally approximated current distribution is to the order to $\sqrt{\epsilon_1}\, k_o$ (ϵ_1 is the leading diagonal element of the permittivity matrix), where the gyro frequency may be both smaller or larger than the plasma frequency. However this approximation does not apply to current distributions along the insulated antenna. The present calculations are also compared with earlier work on antenna impedances.

DD FORM 1 JAN 64 1473

Unclassified
Security Classification

14. KEY WORDS	LINK A		LINK B		LINK C	
	ROLE	WT	ROLE	WT	ROLE	WT
ANTENNA IMPEDANCE PLASMA LATERS IONOSPHERE MAGNETOIONIC MEDIUM						

INSTRUCTIONS

1. ORIGINATING ACTIVITY: Enter the name and address of the contractor, subcontractor, grantee, Department of Defense activity or other organization *(corporate author)* issuing the report.

2*a*. REPORT SECURITY CLASSIFICATION: Enter the overall security classification of the report. Indicate whether "Restricted Data" is included. Marking is to be in accordance with appropriate security regulations.

2*b*. GROUP: Automatic downgrading is specified in DoD Directive 5200.10 and Armed Forces Industrial Manual. Enter the group number. Also, when applicable, show that optional markings have been used for Group 3 and Group 4 as authorized.

3. REPORT TITLE: Enter the complete report title in all capital letters. Titles in all cases should be unclassified. If a meaningful title cannot be selected without classification, show title classification in all capitals in parenthesis immediately following the title.

4. DESCRIPTIVE NOTES: If appropriate, enter the type of report, e.g., interim, progress, summary, annual, or final. Give the inclusive dates when a specific reporting period is covered.

5. AUTHOR(S): Enter the name(s) of author(s) as shown on or in the report. Enter last name, first name, middle initial. If military, show rank and branch of service. The name of the principal author is an absolute minimum requirement.

6. REPORT DATE: Enter the date of the report as day, month, year, or month, year. If more than one date appears on the report, use date of publication.

7*a*. TOTAL NUMBER OF PAGES: The total page count should follow normal pagination procedures, i.e., enter the number of pages containing information.

7*b*. NUMBER OF REFERENCES: Enter the total number of references cited in the report.

8*a*. CONTRACT OR GRANT NUMBER: If appropriate, enter the applicable number of the contract or grant under which the report was written.

8*b*, 8*c*, & 8*d*. PROJECT NUMBER: Enter the appropriate military department identification, such as project number, subproject number, system numbers, task number, etc.

9*a*. ORIGINATOR'S REPORT NUMBER(S): Enter the official report number by which the document will be identified and controlled by the originating activity. This number must be unique to this report.

9*b*. OTHER REPORT NUMBER(S): If the report has been assigned any other report numbers *(either by the originator or by the sponsor)*, also enter this number(s).

10. AVAILABILITY/LIMITATION NOTICES: Enter any limitations on further dissemination of the report, other than those imposed by security classification, using standard statements such as:

(1) "Qualified requesters may obtain copies of this report from DDC."

(2) "Foreign announcement and dissemination of this report by DDC is not authorized."

(3) "U. S. Government agencies may obtain copies of this report directly from DDC. Other qualified DDC users shall request through

_____."

(4) "U. S. military agencies may obtain copies of this report directly from DDC. Other qualified users shall request through

_____."

(5) "All distribution of this report is controlled. Qualified DDC users shall request through

_____."

If the report has been furnished to the Office of Technical Services, Department of Commerce, for sale to the public, indicate this fact and enter the price, if known.

11. SUPPLEMENTARY NOTES: Use for additional explanatory notes.

12. SPONSORING MILITARY ACTIVITY: Enter the name of the departmental project office or laboratory sponsoring *(paying for)* the research and development. Include address.

13. ABSTRACT: Enter an abstract giving a brief and factual summary of the document indicative of the report, even though it may also appear elsewhere in the body of the technical report. If additional space is required, a continuation sheet shall be attached.

It is highly desirable that the abstract of classified reports be unclassified. Each paragraph of the abstract shall end with an indication of the military security classification of the information in the paragraph, represented as *(TS)*, *(S)*, *(C)*, or *(U)*.

There is no limitation on the length of the abstract. However, the suggested length is from 150 to 225 words.

14. KEY WORDS: Key words are technically meaningful terms or short phrases that characterize a report and may be used as index entries for cataloging the report. Key words must be selected so that no security classification is required. Identifiers, such as equipment model designation, trade name, military project code name, geographic location, may be used as key words but will be followed by an indication of technical context. The assignment of links, rules, and weights is optional.